THE JOURNAL OF BIOLOGICAL CHEMISTRY

Vol. 260, No. 10, Issue of May 25, pp. 6449-6458, 1985
Printed in U.S.A.

2.8-Å Structure of Penicillin-sensitive D-Alanyl Carboxypeptidase-transpeptidase from *Streptomyces* R61 and Complexes with β-Lactams*

(Received for publication, November 2, 1984)

Judith A. Kelly, James R. Knox, Paul C. Moews, Gilbert J. Hite‡, John B. Bartolone, and Haiching Zhao

From the Biological Sciences Group, ‡School of Pharmacy, and Institute of Materials Science, The University of Connecticut, Storrs, Connecticut 06268

Bernard Joris, Jean-Marie Frère, and Jean-Marie Ghuysen

From the Service de Microbiologie, Faculte de Medecine, Universite de Liege, Sart Tilman, 4000 Liege, Belgium

The crystallographic structure of the penicillin-sensitive D-alanyl carboxypeptidase-transpeptidase from *Streptomyces* R61 has been solved to 2.8-Å resolution. The 38,000-dalton serine peptidase has two regions of secondary structure, an α/β cluster, and a region which contains five helical segments. The β sheet is composed of five β strands. The tertiary structure has no homology with the classic serine proteases or with the zinc carboxypeptidases. The binding at a common site of three types of β-lactam (a penicillin, a cephalosporin, a monocyclic β-lactam) and a desazacyclobutanone has been observed in Fourier difference maps. The binding site sequence is Val-Gly-Ser-Val-Thr-Lys. The β-lactam ring lies near the enzyme's catalytic serine at position 37, and the C3 substituent of a cephalosporin falls near lysine 40.

The biosynthesis of bacterial cell wall peptidoglycan is catalyzed and controlled in its final stages by a class of enzymes which act on *x*-D-alanyl-D-alanine peptide appendages of *N*-acetylmuramyl-*N*-acetylglucosyl polysaccharides (Georgopapadakou and Sykes, 1983; Ghuysen *et al.*, 1984; Waxman and Strominger, 1983). The enzymes, after removing the COOH-terminal D-alanine, use the new carbonyl to form a peptide bond to an amino acceptor group of a peptide on a neighboring polysaccharide. This transpeptidation produces a cross-linked cell wall network.

Enzyme + *R*-D-Ala-D-Ala-COOH
→ enzyme-CO-Ala-*R* + D-Ala-COOH

Enzyme-CO-Ala-*R* + *R'*-NH_2 → *R'*NHCO-Ala-*R* + enzyme

Some of these enzymes are bifunctional in that they can also use water as the acceptor in step 2 and so act as D-alanyl-carboxypeptidases as well as D-alanyl-transpeptidases. Yet others function solely as D-alanyl-carboxypeptidases, perhaps to limit or control the degree of cross-linking.

Wall biosynthesis is inhibited by antibiotics of the β-lactam family (penicillins and cephalosporins). The β-lactam is able, because of a structural resemblance to the D-alanyl-D-alanine segment, to compete in step 1 to form a transient penicilloyl-enzyme complex. A goal in β-lactam chemistry is to improve the stability of such complexes and to design efficient compounds (high acylation and low deacylation rates) which are resistant to inactivation by β-lactamases. It is therefore useful to determine the geometry of the enzymic β-lactam-binding site and to examine complexes of the enzyme with β-lactams.

A bifunctional, β-lactam-sensitive, D-alanyl-carboxypeptidase-transpeptidase from *Streptomyces* R61 has been chemically and kinetically characterized (Ghuysen *et al.*, 1979, 1980, 1984; Georgopapadakou *et al.*, 1981). Its peptidase activity and β-lactam binding are serine-dependent. However, its rate of inactivation by serine inhibitors is considerably smaller than that of the classic serine proteases, and it is not inhibited by histidine-directed reagents. The molecule is a single polypeptide chain of 38,000 daltons. It contains approximately 350 residues, and the determination of primary structure is 50% completed. Reports of the preliminary crystallography of the enzyme have appeared (Knox *et al.*, 1979; Kelly *et al.*, 1982). Here we present details of the structure analysis at 2.8-Å resolution and results of chemical modification experiments and β-lactam binding studies. The x-ray analysis is continuing to 1.6-Å resolution.

EXPERIMENTAL PROCEDURES

Crystal Growth

Crystals of *Streptomyces* R61 carboxypeptidase/transpeptidase were grown from enzyme purified to 95% homogeneity by J.-M. Ghuysen and J.-M. Frere at the Universite de Liege, Belgium. Lyophilized enzyme was dissolved in 15% (w/v) polyethylene glycol (M_r 8000) in 50 mM phosphate buffer at pH 6.8 to a final concentration of 20 mg/ml. After centrifugation, 20-μl drops of the protein solution were suspended from silanized glass slips over 1-ml reservoirs of 20% PEG[1] solution at 20 °C. Crystals (up to 0.7 mm in length) usually appeared in 3 weeks without seeding, and they could be easily transferred to and maintained in 30% glycol at pH 6.8. Larger crystals (1.2 × 0.8 × 0.7 mm) could be grown by macroseeding in fresh enzyme solution.

* This research was supported by the National Institutes of Health (AI-16702 to J. R. K., AI-13773 to G. J. H., AI-13364 to J. M. G., and S10-RP01955-01 to J. A. K.), North Atlantic Treaty Organization (SA. 5-2-05RG to J. A. K.), the Fonds de la Recherche Scientifique Medicale Brussels (3.4507.83), and a Belgian Action concertee (79/83-I1) to J. M. G. and, in part, by the Burroughs-Wellcome Co., Lilly, Hoffmann-LaRoche, and Merck Sharp and Dohme. The costs of publication of this article were defrayed in part by the payment of page charges. This article must therefore be hereby marked "*advertisement*" in accordance with 18 U.S.C. Section 1734 solely to indicate this fact.

[1] The abbreviations used are: PEG, polyethylene glycol; DFP, diisopropyl fluorophosphate; MIR, multiple isomorphous replacement.

X-ray Analysis

For x-ray photography and diffractometry, crystals were sealed in quartz capillaries. Precession photographs showed the crystals are orthorhombic with a = 51.1 Å, b = 67.4 Å, c = 102.8 Å with space group $P2_12_12_1$. The calculated volume/dalton ratio is 2.33 for an assumed M_r 38,000 and 1 molecule/asymmetric unit. The 16,954 intensities ($\pm 2\theta$) to 2.8-Å resolution were collected at 19 °C with nickel-filtered copper radiation on a 4-circle Picker diffractometer. Of these, 92% were above background by three times their estimated error. A partial-peak ω step scan was used in which 4-s counts were taken at each of seven ω settings 0.02° apart. Crystal alignment and deterioration were monitored by counting three standard reflections every 300 reflections. Intensities of native data usually dropped less than 16% during a 192-h data collection period. Derivative data often decayed up to 20%. A 2θ-dependent background correction, based on measurements at an absorption minimum, was applied (Hill and Banaszak, 1973). An empirical cylindrical absorption correction was made as a function of φ near χ 90°. The absorption correction varied from 1.3 to 1.5. For heavy-atom derivatives, Friedel mates were measured at -2θ in groups of 50 reflections.

Preparation of Heavy-atom Derivatives

Enzyme crystals held in 30% PEG solution were exposed to heavy-atom compounds at 2.5–10 mM final concentration at pH 6.8 for 24–100 h. Compounds found useful for phasing were potassium uranyl pentafluoride, methyl mercury chloride, sodium platinum hexachloride, and 3-isothiocyanato-4-iodobenzenesulfonic acid. Details are given under "Results and Discussion."

Preparation of Enzyme-β-Lactam Complexes

o-Iodobenzamidopenicillanic acid and the cyclobutanone, 6,6-dichloro-4-desaza-2,2-didesmethylpenicillanic acid (Tomczuk, 1980; Tomczuk *et al.*, 1983), cephalosporin C (Lilly), and the monocyclic β-lactam SQ-26,324 (Squibb) were dissolved in the phosphate-buffered 30% PEG solution at concentrations shown in Table III. Enzyme crystals were exposed to the β-lactam solutions at room temperature for the soak times indicated in Table III. Crystals were not washed with β-lactam-free PEG solution before x-ray analysis.

Preparation of Chemically Modified Crystals

Diisopropyl Fluorophosphate (DFP)—Under suitable safety precautions, a crystal of *Streptomyces* R61 carboxypeptidase/transpeptidase was reacted for 48 h at room temperature with 10 mM DFP at pH 6.8 in 30% PEG, 50 mM phosphate buffer. Over a 48-h period prior to reaching the final concentration of 10 mM, the crystal was exposed to small increasing concentrations of the reagent in order to prevent crystal cracking.

3-Isothiocyanato-4-iodobenzenesulfonate—This iodinated Edman reagent, kindly provided by G. A. Petsko (Massachusetts Institute of Technology), was reacted at 10 mM with a crystal for 72 h at pH 6.8 in the 30% PEG-holding solution. The crystal was washed for 8 h with reagent-free PEG solution.

Methylglyoxal—A crystal was reacted for 48 h at room temperature with 15 mM methylglyoxal at pH 6.8 in the 30% PEG-holding solution. Prior to this reaction, the crystal was prereacted for 6 days with smaller concentrations of the reagent.

Iodine—An iodination procedure of Sigler (1970) employing KI and I_2 was used to label tyrosine and possibly histidine residues in the crystalline enzyme (no free cysteine is present). The crystals became deep red as the concentration of fresh I_3^- reactant was increased to 20 mM over an 8-day period in the dark at pH 6.8. After this period, unreacted iodine was washed from the crystal until the color disappeared.

Enzyme Activity Determination

The activity of the enzyme was determined using diacetyl-L-Lys-D-Ala-D-Ala as substrate and the D-amino acid oxidase procedure for the determination of D-alanine (Frère *et al.*, 1976b).

Proteolytic Digestion and Sequence Determination

One hundred nanomoles of enzyme were reacted during 60 min at 37 °C with a 20-fold excess of β-iodopenicillanate (Pfizer) in 250 μl of 10 mM sodium phosphate buffer, pH 7.4. The excess reagent was removed by filtration on Sephadex G-15 and the fractions containing the acyl-enzyme freeze-dried. The dry material was dissolved in 1.0 ml of 10 mM NH_4HCO_3 containing 0.1 mM $CaCl_2$ and 2 M urea. Trypsin (400 μg) was added, and the mixture was incubated at 37 °C for 1 h. The labeled peptide was purified on Sephadex G-25 and a reverse-phase high performance liquid chromatography column as described by Joris *et al.* (1984) by monitoring the absorbance of eluates at 315 nm, a wavelength characteristic of the dihydrothiazine chromophore obtained after acylation of the active site serine by β-iodopenicillanate.[2] Dansylation of the peptide thus obtained indicated only one NH_2-terminal residue (Val). The sequence was determined using the microdansyl-Edman method (Bruton and Hartley, 1970).

RESULTS AND DISCUSSION

Heavy-atom Derivatives—Four heavy-atom compounds listed in Table I were found to produce significant intensity changes with less than 0.2% cell constant changes. Initial heavy-atom coordinates for major sites were determined from three-dimensional Patterson maps based on coefficients F_H^2 which included anomalous dispersion differences (Matthews, 1966):

$$F_H^2 = F_P^2 + F_{PH}^2 - 2F_PF_{PH}(1 - (wk^{-1}(F_{PH}^+ - F_{PH}^-)/2F_P)^2)^{1/2} \quad (1)$$

with the weighting factor $w = 0.75$; the ratio of the imaginary-to-real scattering k was calculated from tabulated scattering factors in the International Tables for X-ray Crystallography (1968). Derivative and native structure factors were scaled so the quantity $\Sigma(|F_P| - |F_{PH}|)^2$ was minimized, where

$$F_{PH} = S \times F'_{PH} \times \exp - (h^2u_1 + k^2u_2 + l^2u_3 + klu_4 + hlu_5 + hku_6) \quad (2)$$

S is the scale factor, and u_i are parameters to correct the measured derivative structure factor F'_{PH} for anisotropic disorder which may be induced by the heavy-atom substitution (Eklund *et al.*, 1981). The scaling method was found useful in removing heavy-atom ghost peaks from the native electron density map.

Harker peaks in the platinum hexachloride Patterson map are shown in Fig. 1. A vector set consistent with a single site was seen about eight times background. The Patterson maps for the uranyl and mercury derivatives were also easily interpretable. Minor heavy-atom sites were found in a series of difference Fourier maps. Atomic positions, occupanices, and temperature factors were refined by a full-matrix least-squares procedure based on all three-dimensional data to 2.8-Å resolution. Additional cycles of heavy-atom refinement were later alternated with phase calculation (see below) to give the final heavy-atom parameters in Table I. To confirm minor sites and to establish the origin of one derivative relative to another, cross-Fourier syntheses were calculated in which the structure factor differences of each derivative were phased from the coordinates of the single-site platinum derivative.

Protein Phase Angles—The method of Blow and Crick (1959) was used to calculate protein phase angles. The phase probability was evaluated at 5° intervals. A reiterative program due to M. G. Rossmann (Adams *et al.*, 1969) allowed a cycle of phasing to be alternated with several cycles of heavy-atom refinement. The calculation included the use of anomalous dispersion differences from three derivatives to 2.8-Å resolution. The data for the platinum derivative were terminated at 4.5 Å. Results from the phasing procedure are shown in Table II. Estimates of the error in the isomorphous and anomalous differences were refined during phasing. Final anomalous difference errors were produced which were ½ to ⅓ of the isomorphous difference errors. For all derivatives except the benzene sulfonate, the lack-of-closure errors are

[2] B. Joris, J.-M. Frère, and J.-M. Ghuysen, unpublished results.

TABLE I

Heavy-atom parameters from least-squares refinement

Derivative	Soak conditions	$R(F)_{obs}$[a]	Site	Fractional coordinates			Occupancy	Shape factor[b]	$R(LS)$[c]
				x	y	z			
$K_3UO_2F_5$	5 mM, 72 h	0.092	U1	0.1313	0.3665	0.2081	59.4	19.7	0.501[d]
			U2	0.6145	0.3604	0.0289	8.5	19.8	0.482
			U3	0.2374	0.2261	0.4004	8.9	27.3	
Na_2PtCl_6	5 mM, 95 h	0.090	Pt	0.0293	0.1585	0.1274	39.9	28.5	0.459
CH_3HgCl	2.5 mM, 69 h	0.115	Hg1	0.0705	0.1895	0.6872	56.7	15.3	0.528
			Hg2	0.1966	0.3072	0.2320	10.8	37.6	
3-Isothiocyanato-4-iodobenzenesulfonate	10 mM, 72 h	0.078	I	0.4500	0.8235	0.4312	16.3	17.0	0.660
			SO_3^-	0.3571	0.7923	0.3852	16.9	14.5	

[a] $R(F)_{obs} = \Sigma|\Delta F_{obs}|/\Sigma|F_P|$, where $\Delta F_{obs} = |F_{PH}| - |F_P|$. $|F_{PH}|$ and $|F_P|$ are the measured structure amplitudes of the derivative and native protein in electrons.

[b] The shape factor (Å^2) is composed of both temperature factor sinθ dependence and atom scattering factor sinθ dependence.

[c] $R(LS) = \Sigma||F_H| - |f_H||/\Sigma|F_H|$, where $|F_H|$ is the Matthews' combination difference of Equation 1 and $|f_H| = (A^2 + B^2)^{1/2}$ for the heavy-atom constellation.

[d] $R(LS) = 0.501$ for U1 alone; 0.482 for all sites.

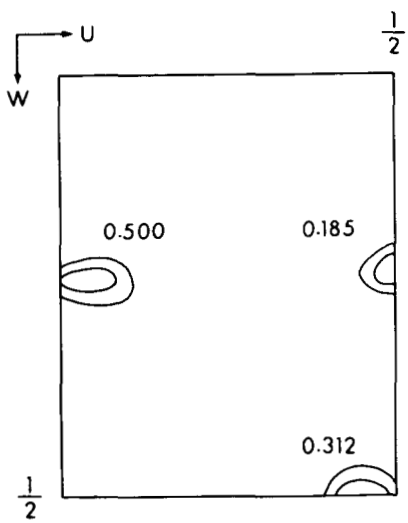

FIG. 1. **Composite of three Harker peaks in Patterson map of platinum hexachloride derivative.** Contours are at 1/25 of origin peak. The v coordinate of each peak is indicated.

TABLE II

Summary of phasing results for 2.8-Å data

The average F_P is 459 electrons. The mean figure of merit for all data is 0.72. r.m.s., root mean square.

Derivative	ΔF_{obs}	f_H	Closure[a]	R_{mod}[b]	$R_{centric}$[c]	$R(K)$[d]
	r.m.s.					
$K_3UO_2F_5$	48.0	54.5	30.9	0.48	0.65	0.06
Na_2PtCl_6	69.0	63.5	45.0	0.62	0.57	0.07
CH_3HgCl	54.6	60.3	50.9	0.76	0.73	0.08
3-Isothiocyanato-4-iodobenzenesulfonate	49.6	36.9	40.7	0.98	0.77	0.06

[a] Root mean square closure = $[\Sigma(|F_{PH}| - |F_P + f_H|)^2/n]^{1/2}$, where n is the number of reflections.

[b] $R_{mod} = \Sigma|\text{closure}|/\Sigma|f_H|$.

[c] $R_{centric} = \Sigma||F_{PH} - F_P| - |f_H||/|\Sigma|F_{PH} - F_P|$.

[d] $R(K) = \Sigma||F_{PH}| - |F_P + f_H||/\Sigma|F_{PH}|$.

less than the root mean square heavy-atom f_H; the ratio of the two is reflected in the R_{mod} values. The mean figure of merit for all 8484 data to 2.8-Å resolution is 0.72.

Native Electron Density Map—Centroid phases were used to calculate the electron density map at 2.8-Å resolution. The F_P were weighted by their figure of merit m. Initially, a minimap composed of stacked xz sections was calculated at a scale of 3.2 Å/cm. The first contour was drawn at 0.2 eÅ^{-3}, the error level is 0.03 eÅ^{-3} estimated from $(1\text{-}m^2)$ F_P^2 summations. Large solvent areas and the boundary of a single molecule were apparent. The right-handedness of α-helices in the map confirmed the choice of absolute configuration during phasing. A sheet of five extended β strands was also seen. A completely connected polypeptide chain could not be traced in its entirety in this first map. For those portions of the polypeptide which were clearly seen, coordinates at approximately 4-Å intervals along the backbone chain were recorded. These coordinates and the electron density map were transferred to an MMS-X interactive graphics system in the laboratory of M. N. G. James (University of Alberta). The use of depth-cued three-directional contouring greatly facilitated map interpretation and further chain tracing. The quality of the map can be observed in Fig. 2, which shows a segment of α-helical electron density as pictured on the MMS-X screen. Main chain carbonyl density and side chain density off the helix core are readily seen in the figure. In all, eight segments of helix and five β strands were fitted with idealized secondary structures of polyalanine in this early analysis. The linkages between the secondary structures were not clear in some places. The directions of a few helices and β strands were later found to be incorrect. About 80% of the length of the 350-residue molecule was accounted for at this point.

In an attempt to enhance further the quality of the map, the density-modification method of Bhat and Blow (1983) was applied. The multiple isomorphous replacement (MIR) map was calculated on a 0.75-Å grid. The incomplete atomic model was used to provide guide points, and these were expanded to include all "well-connected density points" using the criteria of Bhat and Blow (1983). The remainder of the map was assumed to be solvent and was set to a constant electron density. The modified density was back-transformed to obtain phases which were combined with the MIR phases using the Hendrickson and Lattman (1970) COMBINE program. Two iterations of this process were carried out, and new phases resulted which, on average, differed 24° from the MIR phases. Only slight improvement could be detected in the enhanced map, possibly because the MIR phases were rather good at the start of the procedure.

To confirm the chain tracing and to re-examine ambiguous portions, use was made of a new algorithm for map display

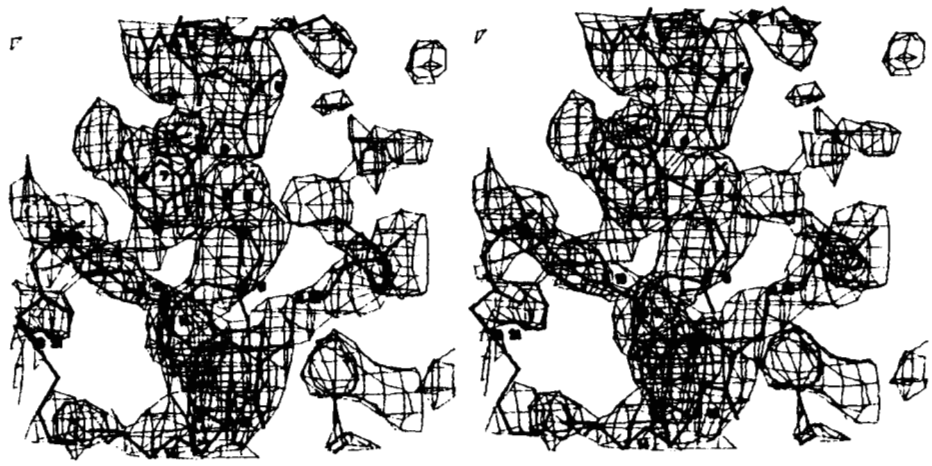

FIG. 2. **Stereoview of electron density and polypeptide model in C helix at 2.8-Å resolution.**

developed at the University of North Carolina (Williams, 1982). The graphics algorithm (GRINCH) represents electron density not by conventional contour surfaces, but rather by branching ridge lines connecting maxima in the density function. With a considerable reduction in the number of lines computed, it is possible in the initial stages to search for the molecule in a global view of the entire cell or asymmetric unit. In the ideal situation, the ridge line network would produce the usual stick diagram of a protein molecule. Because of the abbreviated representation of the density in this new program, much larger segments of the density map can be displayed without the obscuring effect of the full contour representation. Thus, GRINCH was successful in revealing several tracing errors including errors in secondary structure directions. Polypeptide fragments not seen in earlier analyses were also evident so that the complete chain length, except for 13 NH_2-terminal residues, could be followed with confidence. The result of the GRINCH tracing of backbone density is shown in Fig. 3. The complete chemical sequence is not yet known, but many side chains (not shown) could be fitted in the GRINCH tracing. As larger fragments have become available from the chemical sequencing, attempts have been made to position them in the model by aligning the chemical and crystallographic sequences. It is hoped that this will minimize the need for overlaps in the chemical sequence work. Atom coordinates of the crystallographically determined sequence have been deposited in the Brookhaven Protein Data Bank (Bernstein *et al.*, 1977). In the coordinate listing and in this paper, a tentative residue numbering scheme is used which is subject to revision when the chemical sequencing is completed.

The Secondary and Tertiary Structure—About 40% of the molecule is composed of secondary structure. Eight helical segments, each three-to-five turns in length, comprise 75% of the secondary structure, and five β strands, each approximately 6 residues long, account for 25%. As seen in Fig. 4, the connectivity of structure elements from the NH_2 to COOH terminus is αA-(βA-βB-αB-βC-αC-βD-βE-αD)-αE-αF-αG-αH. The molecule falls into a new class of proteins with a region of α/β structure and an area that is all helical (Levitt and Chothia, 1976). The group of structure elements enclosed by parentheses is seen in the right of Fig. 4; it is a close cluster of the parallel-α/mixed-β type (Richardson, 1981). The linkages in the cluster can be represented by Richardson's notation as +1, +1x, +1x, +1 or as ↓⌒⌒⌒↑, in which there are two right-handed crossovers from parallel β strands to parallel α-helices. The β sheet contains both parallel and antiparallel strands, and it has the common left-handed twist (as viewed perpendicular to the strands) with a rather small Ω angle of about 10°. The less stable parallel strands βB-βC-βD are sequestered in the middle of the β sheet away from solvent; they are protected by two parallel helices αB and αC on one face and by a longer helix αD which runs across the back face of the sheet. Helices αB and αC are each −15 °Ω to the β strands, and helix αD lies at −40 °Ω to the strands. The near parallelism ($\Omega < 10°$) of αB and αC gives rise to an unfavorable alignment of dipole moments which, however, is countered by opposite moments of the nearest β strands (Hol *et al.*, 1981). In the left portion of the molecule is a loose clustering of the remaining five helices αA, αE, αF, αG, and αH, each at a large oblique angle to its neighbors.

Whether the two clusters in the *left* and *right* of Fig. 4 can properly be called domains is not clear. A space-filling picture (Fig. 5) shows an apparently compact folding. A more quantitative method of searching for domain folding is to calculate a neighborhood correlation (Schulz and Schirmer, 1979)

$$c(\mathrm{i}) = \sum 1/d(i,k)$$

$$6 \leq |i - k| \leq 25$$

where $d(i,k)$ is the distance between α-carbon atoms separated by at least 6 and no more than 25 positions. A plot of $c(i)$ *versus* i for this structure shows three maxima, the most extensive of which corresponds to residues 125–270 identified previously as the α/β cluster (*right* of Fig. 4). This α/β cluster is joined to the remainder of the molecule by only two polypeptide strands, but the cluster fits snugly against it and consequently is not easily recognized in Fig. 5.

The tertiary structure was qualitatively examined for homology with other crystallographic structures, especially serine proteases and the zinc-containing carboxypeptidases, but no homology was evident. One case in particular, the *Streptomyces albus* G D-alanyl-carboxypeptidase, was examined carefully because it is highly specific for the D-alanyl-D-alanine linkage, as is the title enzyme. Its sensitivity to β-lactams, however, is very low. It is 22,000 daltons, contains an NH_2-terminal α-helical cluster, and has four β strands near the hydrolysis site in a COOH-terminal domain (Dideberg *et al.*, 1982). It bears little structural resemblance to the larger *Streptomyces* R61 D-alanyl-carboxypeptidase-transpeptidase described here. Neither is there any similarity in tertiary folding of the *Streptomyces* R61 carboxypeptidase/transpeptidase and either phage or hen lysozyme, which, like the carboxypeptidase/transpeptidase, interacts with bacterial peptidoglycan and, in the case of hen lysozyme, even binds penicillin, although only at high concentration (Corran and Waley, 1975; Felsenfeld and Handschumaker, 1967; Johnson,

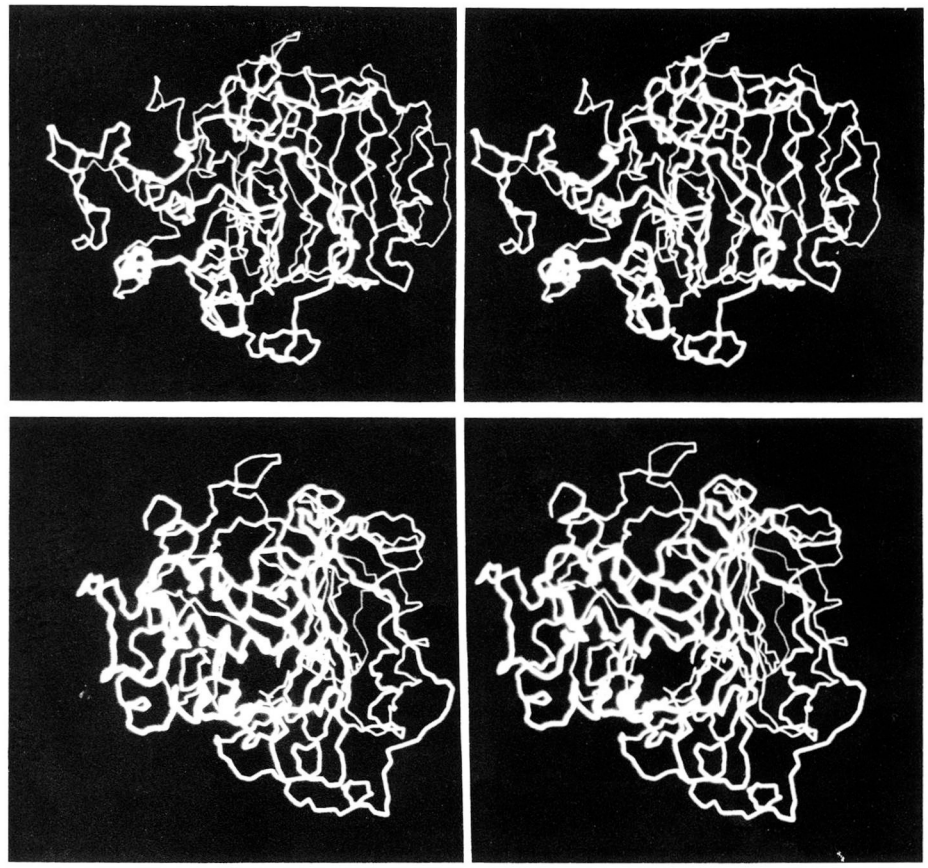

FIG. 3. **Stereoviews from GRINCH representation of main chain electron density.** Cephalosporin C is positioned in the β-lactam-binding site. *Top*, front view; *bottom*, left-side view.

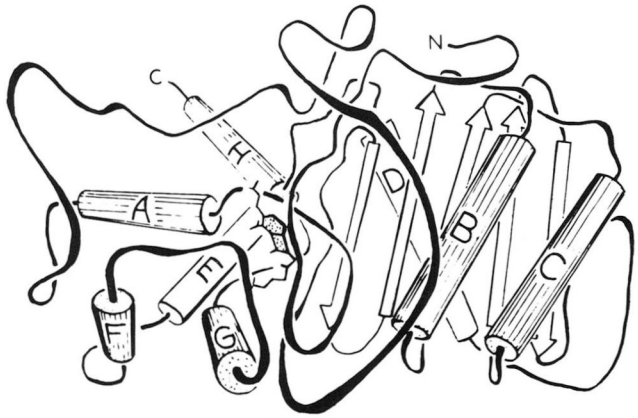

FIG. 4. **Main chain folding schematic of *Streptomyces* R61 carboxypeptidase/transpeptidase.** *Cylinders* and *arrows* represent α-helices and β strands, respectively. Amino and carboxyl termini are indicated. Approximate residue numbering in each secondary structure element is: αA(42–55), βA(150–158), βB(159–167), αB(172–186), βC(189–197), αC(202–214), βD(216–225), βE(227–235), αD(248–265), αE(275–285), αF(288–299), αG(306–321), and αH(341–353). Cephalosporin C is shown in the β-lactam-binding site.

1967). When the *Streptomyces* R61 carboxypeptidase/transpeptidase structure is refined with high resolution x-ray data and the completed sequence, we will search for lysozyme-like saccharide interaction sites which could accommodate *N*-acetylmuramic and *N*-acetylglucosamine moieties. Whether the family of penicillin-inhibited D-alanyl-carboxypeptidase/transpeptidase enzymes is related to the penicillin-destroying β-lactamases has been discussed (Moews *et al.*, 1981; Spratt, 1983; Waxman and Strominger, 1983), and we will comment on this point later.

Difference Maps—To observe the binding of the compounds listed in Table III, electron density difference maps were calculated using the native MIR phases and coefficients $m(|F_M| - |F_P|)$, where F_M is the structure factor of the complexed or chemically modified enzyme. The F_M were scaled to F_P with the same anisotropic method used for the heavy-atom derivative data (see Eqn 2). Acentric data were weighted by $\pi/2$ (Moews and Bunn, 1971). Difference electron densities for selected complexes are shown in Fig. 6. Density peaks (positive or negative) were considered significant only if they were at least 2.5 times background density.

β-Lactam Binding—To locate the antibiotic-binding site, complexes of β-lactams with the crystalline enzyme were prepared by diffusing β-lactams into pregrown crystals. The three β-lactams and the cyclobutanone listed in Table III represent distinctive classes of four-membered ring inhibitors. They have very different chemical structures and kinetic constants with respect to the *Streptomyces* R61 carboxypeptidase/transpeptidase (Ghuysen *et al.*, 1979). Yet, they were all found to bind at a common site which is described in more detail below. The iodinated phenylpenicillin was used in the first low resolution mapping with 4-Å data. It produced ellipsoidal density centered at *xyz* fractional coordinates 0.38 −0.18 0.41. Cephalosporin C, a representative of the large cephalosporin family of β-lactams, was chosen for study because it contains a hydrophilic C7 substituent and has a long half-life of binding (7.5 days) to the *Streptomyces* R61 enzyme (Ghuysen *et al.*, 1979). The envelope of 2.8-Å difference density (Fig. 6, *top*) is consistent with the size and molecular shape of cephalosporin C. A model of cephalosporin C was built based on the correct absolute configuration from crystallographic coordinates (Hodgkin and Maslen, 1961). This model was fitted into the difference density initially as a rigid body and then with the allowed rotations of the C7 side chain. The difference map showed no density for the C3′ side chain

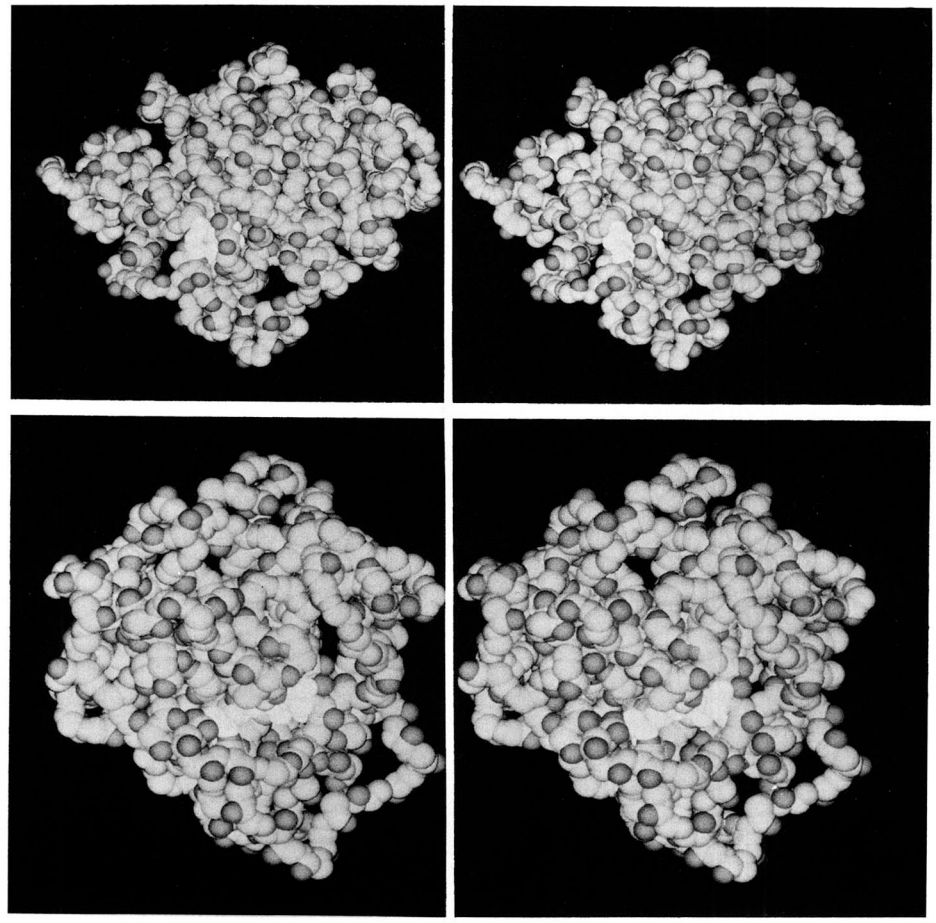

FIG. 5. **Stereoviews of space-filling main chain model of** *Streptomyces* R61 carboxypeptidase/transpeptidase. Side chains are omitted. *Top*, front view generally in the orientation of Figs. 3, *top*, and 4. *Bottom*, left side view similar to Fig. 3, *bottom*.

of the antibiotic. Because opening of the β-lactam bond in cephalosporins is accompanied by elimination of the C3′ leaving group (Boyd, 1982; Faraci and Pratt, 1984), the difference map indicates that an acyl-enzyme complex has likely been isolated in these studies.

The 6,6-dichloro-desazapenicillanic acid was designed to be resistant to hydrolysis by β-lactamases and D-alanyl-transpeptidases (Tomczuk, 1980). Although this cyclobutanone is not antibiotic to growing cells, we find that it is, nevertheless, a competitive inhibitor of this enzyme (K_i = 1 mM) (Tomczuk *et al.*, 1983) and that it binds to the crystalline enzyme. Thus, the electron pair on a β-lactam nitrogen may not be essential (Gordon *et al.*, 1981) for recognition of inhibitors by this enzyme. The compound's lack of *in vivo* effectiveness may be due to poor penetration through bacterial membrane barriers, to chemical instability in the presence of amines, or to its inability to acylate target enzymes. The two chlorine atoms at one end of the cyclobutanone enabled us to confirm the bicyclic ring structure is oriented within the 4-Å density map in the same way as cephalosporin C is oriented, although a 2-Å translation of the cyclobutanone relative to the cephalosporin is necessary to fit the map density.

The monocyclic β-lactam SQ-26,324 represents a series of newly discovered antibiotics which lack the 5- or 6-membered heterocyclic ring adjacent to β-lactam ring (Sykes *et al.*, 1981). It is similar to all other β-lactams in having a negative functionality which is one atom removed from the β-lactam nitrogen. The low resolution (4 Å) difference map for the benzyl monobactam shows two major peaks, one at the same general site occupied by other β-lactams, the other 30 Å away on the left surface of the enzyme (as shown in Fig. 4) and apparently ionically bound near tyrosine 69.

Enzymic Side Chain Labels—It was necessary to show that the β-lactam-binding site identified crystallographically contains the same catalytic groups identified by Frère *et al.* (1976a) and Georgopapadakou *et al.* (1981) in their chemical inhibition studies of the *Streptomyces* R61 enzyme in solution. We therefore reacted the crystals with the same serine-directed and amine-directed reagents they used in their studies. Because visualization of amino acid residues at 2.8-Å resolution is not uniformly clear along the polypeptide chain, chemical labeling by these and other reagents helped also to assign or confirm parts of the amino acid sequence.

DFP is an electrophile commonly used to inhibit serine proteases. The DFP Fourier difference map is featureless except for a single region of positive density near serine 37 in the β-lactam-binding site. The DFP density overlaps a part of the positive density in the cephalosporin C difference map. In solution, the DFP reagent was shown to inhibit penicillin binding and peptidase activity of this enzyme (Ghuysen *et al.*, 1979; Georgopapadakou *et al.*, 1981). We conclude that the serine labeled with DFP in the crystal is the penicillin-sensitive catalytic serine. A single negative density peak is also present in the DFP map. It is about 3.5 Å from the serine oxygen and is within 1 Å of the only negative peak seen in the cephalosporin difference map. The negative peak may represent a water molecule, phosphate buffer ion, or protein group which is displaced during the binding reaction at the serine position.

The amine-directed 3-isothiocyanato-4-iodo-benzenesulfonate labeled an as yet unidentified side chain (currently numbered 42) at the β-lactam-binding site. The side chain is 5 residues from the reactive serine 37, yet it folds within 3 Å of the serine. The Edman reagent was expected to label the

TABLE III

Complexes and chemical modifications examined by Fourier difference maps

Compound	Soak conditions	Data resolution	$R(F)_{obs}$[a]	Found at
		Å		
o-Iodobenzamido-penicillanic acid[b]	40 mM, 36 h	4.0	0.065	β-Lactam site
Cephalosporin C[c]	15 mM, 48 h	2.8	0.074	β-Lactam site
Cyclobutanone[d]	20 mM, 17 h	4.0	0.169	β-Lactam site
Monobactam SQ-26,324[e]	10 mM, 20 h	4.0	0.072	β-Lactam site
Diisopropylfluorophosphate	10 mM, 48 h	2.8	0.136	Serine 37 (β-lactam site)
3-Isothiocyanato-4-iodobenzene-sulfonate	10 mM, 72 h	2.8	0.078	Amino group 42 (β-lactam site)
Methylglyoxal	15 mM, 48 h	2.8	0.122	Lys/Arg 25, amino group 42
Iodine	20 mM 8 days	2.8	0.145	Tyrosines

[a] See Table I for definition.

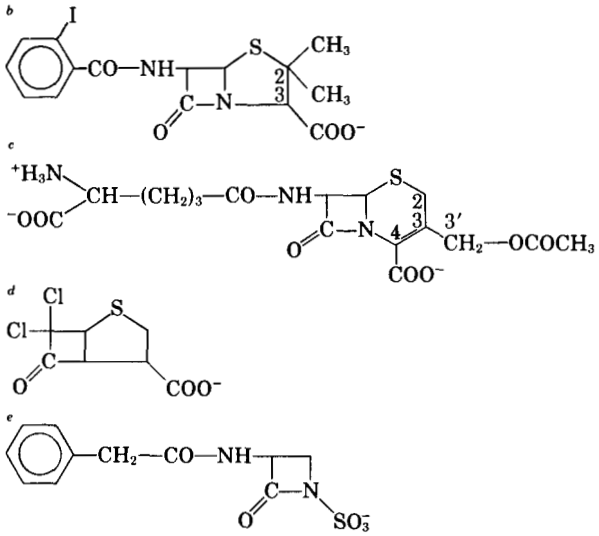

α-amino group at the enzyme's NH_2 terminus, but it either failed to do so or is not seen there because of disorder of the NH_2 terminus. The covalent isothiocyanate label was used for phasing the 2.8-Å data (Table II). Two positive density peaks are resolved in the difference map 7 Å apart and are presumably the iodo and sulfonato substituents.

Another amine-directed reagent, methylglyoxal, produced a Fourier difference map with a cluster of four positive peaks and two negative peaks in the vicinity of the β-lactam site. Two of the positive peaks occur on the periphery of the unidentified side chain 42 which was also labeled by the isothiocyanate reagent. A third positive peak labels lysine or arginine 25, which is about 7 Å from the catalytic serine; the single methylglyoxal peak suggests the residue is lysine. One of the negative peaks in the methylglyoxal map is coincident with the negative peak in the cephalosporin and DFP difference maps. A solvent molecule or buffer ion in this common position would generally lie between the catalytic serine 37 and the labeled lysine/arginine 25 side chain. The remaining positive and negative peaks occur as a close pair near residues valine 38 to threonine 39 and could represent an induced shift of main chain.

Iodine (as KI_3) was used to label tyrosine and possibly histidine residues and to confirm the crystallographic sequencing of amino acids. The data were not used in the phasing procedure. In all, 12 positive peaks and no negative peaks are found in the 2.8-Å difference map. Most of the peaks are on the surface of the molecule. No peaks occur on the surface regions which are in close contact with neighboring molecules, as might be expected. No residues in the β-lactam-binding site are iodine-labeled. Nine of the iodine peaks can be associated with 7 aromatic residues (54, 69, 72, 125, 181, 188, and 328) which had earlier been tentatively identified in the map as tyrosine or phenylalanine. On two of these tyrosines (54 and 72), ortho-disubstitution is seen.

The β-Lactam-binding Site—Flanked on one side by the beginning of the αA helix, at the rear by the βA strand of the β sheet, and at the bottom by the αG helix, the general position of β-lactam binding is seen in Figs. 4 and 5. The direction of approach of the antibiotic to the binding site would most likely be from the upper left corner of Fig. 4. The position and orientation of the cephalosporin C moiety in the binding site was discerned from a Fourier difference map at 2.8-Å resolution. Detailed description of the interaction must await higher resolution data, but the absence of the C3′ group leads us to believe an acylated antibiotic is present. Not surprisingly, the cyclobutanone, which lacks the β-lactam nitrogen and cannot therefore react chemically with the enzyme, was found to penetrate less deeply into the binding site than did cephalosporin C. Amino acid side chains potentially able to contact a β-lactam are in a 20-residue coil of polypeptide in the NH_2-terminal portion of the molecule, generally from residue 25 to 45 (Fig. 7). After encircling the antibiotic, the peptide coil develops into the αA helix, the dipole moment of which (Hol *et al.*, 1981; Sheridan and Allen, 1980) may place a partial positive charge near the β-lactam site. All β-lactams soaked into the crystals bind near serine 37, which is the sole serine labeled in the crystal with the inhibitor DFP. The sequence of the serine peptide, obtained by trypsin digestion of the enzyme labeled in solution with β-iodopenicillanate, is Val-Gly-Ser-Val-Thr-Lys. The crystallographically determined sequence around serine 37 (Table IV and Fig. 7) is thus equivalent to the chemically determined sequence.

One or more active site bases have been proposed to participate in two processes: 1) ionic interaction with a penicillin's C3 or a cephalosporin's C4 carboxyl group or with the terminal

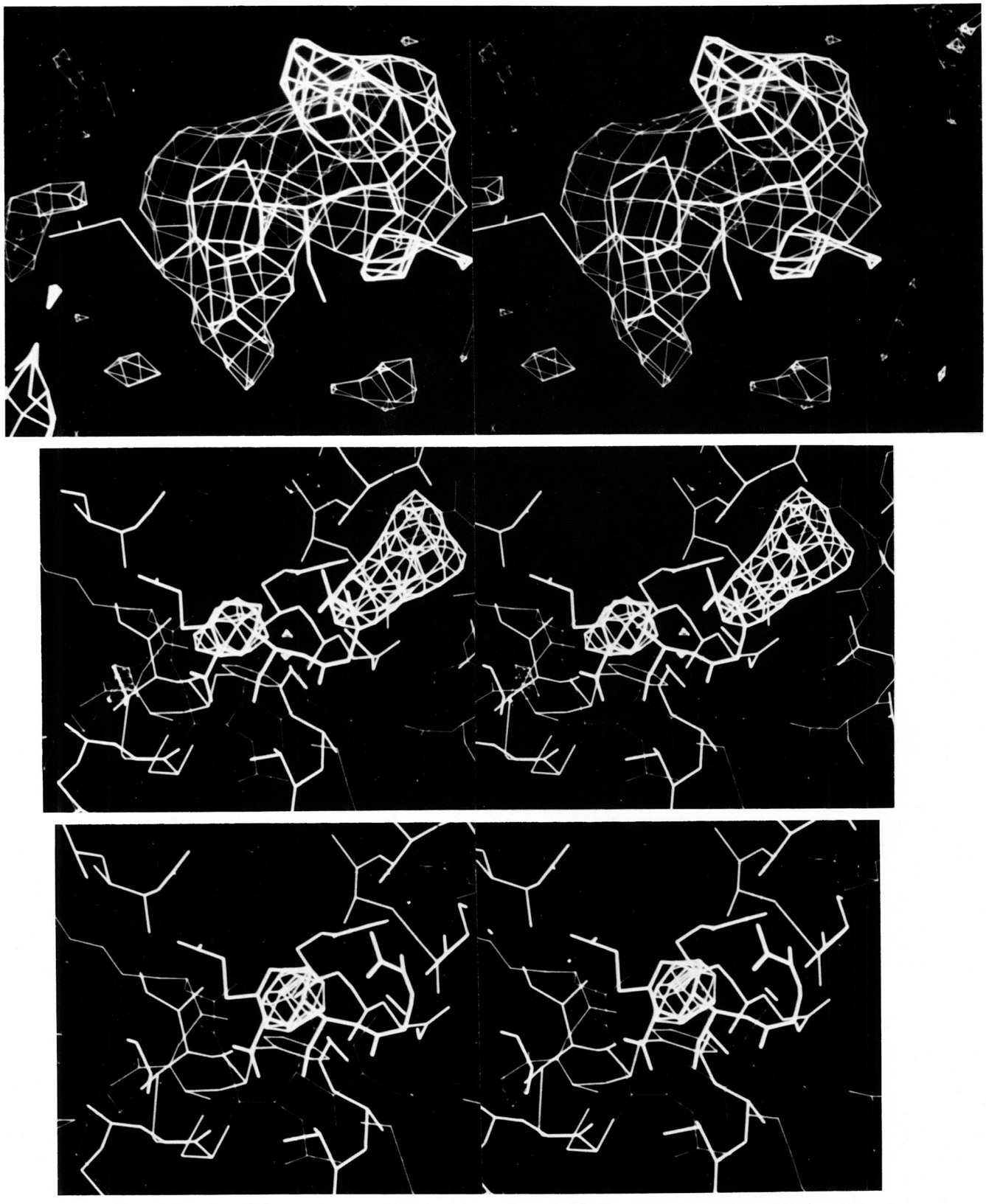

FIG. 6. **Fourier difference maps of β-lactam complexes with *Streptomyces* R61 carboxypeptidase/transpeptidase.** All diagrams include the fitted cephalosporin position for reference. The views are generally from the *bottom left* of Fig. 3, *top*, or 4, *top*. *Top*, cephalosporin C electron density at 2.8-Å resolution. *Center*, 6,6-dichloro-4-desaza-2,2-didesmethylpenicillanic acid density at 4-Å resolution with surrounding protein model. The major features in the difference map are the chloro and carboxy densities, which indicate a shift of the cyclobutanone is necessary relative to the cephalosporin position. A portion of the G helix is seen in the foreground. Serine 37 is at the right rear of the β-lactam. Unknown residue 42 is here represented by the phenylalanine in front of β-lactam. *Bottom*, monobactam SQ-26,324 density at 4-Å resolution. The sulfonate density predominates.

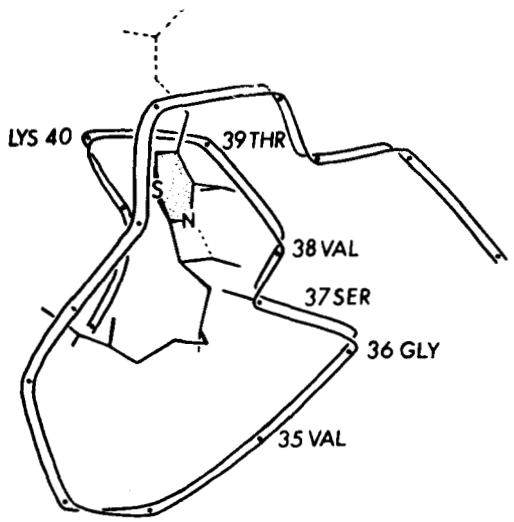

FIG. 7. **A *yz* projection of α-carbon atoms 25–42 (*dots*) showing folding of active site polypeptide around the β-lactam position.** Cephalosporin C is presumed to be covalently bound to the enzyme via serine 37 and is shown with an open β-lactam ring. The leaving group at C3 is not seen in the map and is *drawn dashed.*

TABLE IV

Comparison of binding site sequences in β-lactam-sensitive enzymes

Enzyme	Sequence near reactive serine
CPase/TPase[a] *S.* R61[b]	Phe-Gly-Val-Gly-*Ser*-Val-Thr-*Lys*
CPase *B. stearothermophilis*[c]	Leu-Gly-Ile-Ala-*Ser*-Met-Thr-*Lys*
CPase penicillin-binding protein 5 *E. coli*[d]	Arg-Asp-Pro-Ala-*Ser*-Leu-Thr-*Lys*
TPase penicillin-binding protein 3 *E. coli*[e]	Phe-Glu-Pro-Gly-*Ser*-Thr-Val-*Lys*
β-Lactamase class A *B. licheniformis*[f]	Phe-Ala-Phe-Ala-*Ser*-Thr-Ile-*Lys*
β-Lactamase class C *Enterobacter cloacae* P99[g]	Phe-Glu-Leu-Gly-*Ser*-Ile-Ser-*Lys*

[a] CPase/TPase, carboxypeptidase-transpeptidase.

[b] The first 2 residues were identified only in the crystallographic map; the remaining 6 residues were confirmed by chemically determined sequence.

[c] Yocum *et al.*, 1980. The binding site sequence of the *B. subtilis* carboxypeptidase is similar.

[d] Broome-Smith *et al.*, 1983.

[e] Maruyama *et al.*, 1983.

[f] Ambler, 1980.

[g] Joris *et al.*, 1984.

carboxyl of the D-alanyl-D-alanine substrate (Georgopapadakou *et al.*, 1981) and 2) fragmentation of an enzyme-bound penicilloyl (or cephalosporoyl) moiety at C5–C6 (or C6–C7) prior to deacylation of an acyl-enzyme intermediate (Ghuysen *et al.*, 1984). Relevant to the ionic process, our reaction of the crystals with the inhibitor methylglyoxal resulted in the labeling of lysine/arginine 25 and possibly residue 42, either of which could be the interacting amine identified by Georgopapadakou *et al.* (1981). Lysine 40 was not clearly labeled by methylglyoxal. As to the fragmentation process, we see that lysine 40 is at the top of the binding site, where it is rather far (6 Å) from the C5–C6 (or C6–C7) bond of a β-lactam ring; there, lysine 40 is better positioned to interact with a C3 substituent of a cephalosporin or possibly with its C4 carboxyl group. Residue 42, on the other hand, is much closer to the β-lactam ring position and could participate in either base-mediated process. This unknown residue is within 3 Å of the reactive serine 37 so that a hydrogen-bonded couple could exist. The labeling of residue 42 in the crystal with the isothiocyanate reagent, which is expected to label only primary amines, the failure of residue 42 to react in the crystal with iodine, and the observation by Georgopapadakou and Sykes (1983) that the enzyme in solution is not inhibited by a histidine-directed chloromethyl-ketone substrate analog all suggest residue 42 is an amine other than histidine.

The crystal structures of other penicillin-sensitive enzymes are not yet known, but the *Streptomyces* R61 carboxypeptidase/transpeptidase sequence near the reactive serine 37 shows some homology with the binding-site sequences of D-alanyl-carboxypeptidases and transpeptidases from *Bacilli* and *Escherichia coli* (Table IV). In all cases except penicillin-binding protein 3, the reactive serine is within the first 50–90 residues. The common NH_2-terminal location of the β-lactam-binding site and the recurring Ser-*x*-*x*-Lys pattern in the known D-alanyl-carboxypeptidases and transpeptidases is seen also in the penicillin-destroying β-lactamases of both A and C classes (Ambler, 1980; Knott-Hunziker *et al.*, 1982), the tertiary structures of which are currently under investigation (Charlier *et al.*, 1983 and references therein). Considering the smaller size of some β-lactamases (only 260 residues are sufficient for class A β-lactamases, for example), we note that, under an assumption of structural homology, these β-lactamases would lack a portion of the COOH-terminal domain of helices E, F, G, and H, none of which interact intimately with the β-lactam, but which in the carboxypeptidases could be involved with peptidoglycan binding during wall biosynthesis.

Acknowledgments—We thank M. N. G. James (University of Alberta) for use of the MMS-X graphics system, G. A. Petsko (Massachusetts Institute of Technology) for use of a Vector General 3404 system, and M. E. Pique (University of North Carolina) for generous assistance in using the facilities of the Molecular Graphics Laboratory, a National Institutes of Health National Research Resource.

REFERENCES

Adams, M. J., Haas, D. J., Jeffery, B. A., McPherson, A., Mermall, H. L., Rossmann, M., Schevitz, R. W., and Wonacott, A. J. (1969) *J. Mol. Biol.* **41,** 159–188

Ambler, R. P. (1980) *Philos. Trans. R. Soc. Lond. B Biol. Sci.* **289,** 321–331

Bernstein, F. C., Koetzle, T. F., Williams, G. J. B., Meyer, E. F., Brice, M. D., Rodgers, J. R., Kennard, O., Shimanouchi, T., and Tasumi, M. (1977) *J. Mol. Biol.* **112,** 535–542

Bhat, T. N., and Blow, D. M. (1983) *Acta Crystallogr. Sect. A Cryst. Phys. Diffr. Theor. Gen. Crystallogr.* **39,** 166–170

Blow, D. M., and Crick, F. H. C. (1959) *Acta Crystallogr.* **12,** 794–802

Boyd, D. B. (1982) in *Chemistry and Biology of β-Lactam Antibiotics* (Morin, R. B., and Gorman, M., eds) Vol. 1, pp. 437–545, Academic Press, New York

Broome-Smith, J., Edelman, A., and Spratt, B. G. (1983) in *The Target of Penicillin* (Hakenbeck, R., Holtje, J. V., and Labinschinski, H. eds) pp. 403–407, W. de Gruyter and Co., Berlin

Bruton, C. J., and Hartley, B. S. (1970) *J. Mol. Biol.* **52,** 165–178

Charlier, P., Dideberg, O., Frère, J. M., Moews, P. C., and Knox, J. R. (1983) *J. Mol. Biol.* **171,** 237–238

Corran, P. H., and Waley, S. G. (1975) *Biochem. J.* **149,** 357–364

Dideberg, O., Charlier, P., Dive, G., Joris, B., Frère, J. M., and Ghuysen, J. M. (1982) *Nature (Lond.)* **299,** 469–470

Eklund, H., Samama, J.-P., Wallén, L., Brändén, C.-I., Åkeson, Å., and Jones, T. A. (1981) *J. Mol. Biol.* **146,** 561–587

Faraci, W. S., and Pratt, R. F. (1984) *J. Am. Chem. Soc.* **106,** 1489

Felsenfeld, H., and Handschumacher, R. E. (1967) *Mol. Pharmacol.* **3,** 153–160

Frère, J. M., Duez, C., Ghuysen, J. M., and Vandekerkhove, J. (1976a) *FEBS Lett.* **70,** 257–260

Frère, J. M., Leyh-Bouille, M., Ghuysen, J. M., Nieto, M., and Perkins, H. R. (1976b) *Methods Enzymol.* **44,** 610–636

Georgopapadakou, N. H., and Sykes, R. B. (1983) *Handb. Exp. Pharmacol.* **67,** 1–77

Georgopapadakou, N. H., Liu, F. Y., Ryono, D. E., Neubeck, R., and Ondetti, M. A. (1981) *Eur. J. Biochem.* **115,** 53–57

Ghuysen, J. M., Frère, J. M., Leyh-Bouille, M., Coyette, J., Dusart, J., and Nguyen-Disteche, M. (1979) *Annu. Rev. Biochem.* **48,** 73–101

Ghuysen, J. M., Frère, J. M., Leyh-Bouille, M., Perkins, H. R., and Nieto, M. (1980) *Philos. Trans. R. Soc. Lond. B Biol. Sci.* **289,** 285–301

Ghuysen, J.-M., Frère, J. M., Leyh-Bouille, M., Nguyen-Disteche, M., Coyette, J., Dusart, J., Joris, B., Duez, C., Dideberg, O., Charlier, P., Dive, G., and Lamotte-Brasseur, J. (1984) *Scand. J. Infect. Dis.,* in press

Gordon, E. M., Pluscec, J., and Ondetti, M. A. (1981) *Tetrahedron Lett.* **22,** 1871–1874

Hendrickson, W. A., and Lattman, E. E. (1970) *Acta Crystallogr. Sect. B Struct. Crystallogr. Cryst. Chem.* **26,** 136–143

Hill, E. J., and Banaszak, L. J. (1973) *Acta Crystallogr. Sect. B Struct. Crystallogr. Cryst. Chem.* **29,** 372

Hodgkin, D. C., and Maslen, E. N. (1961) *Biochem. J.* **79,** 393–402

Hol, W. G. J., Halie, L. M., and Sander, C. (1981) *Nature (Lond.)* **294,** 532–536

International Tables for X-ray Crystallography (1968) Vol. 3, p. 215, Kynoch Press, Birmingham, England

Janin, J., and Chothia, C. (1980) *J. Mol. Biol.* **143,** 95–128

Johnson, L. N. (1967) *Proc. R. Soc. Lond. B Biol. Sci.* **167,** 439–440

Joris, B., Dusart, J., Frère, J. M., Van Beeumen, J., Emanuel, E. L., Petursson, S., Gagnon, J., and Waley, S. G. (1984) *Biochem. J.* **223,** 271–274

Kelly, J. A. (1983) in *The Target of Penicillin* (Hakenbeck, R., Holtje, J. V., and Labischinski, H., eds) pp. 387–392, W. de Gruyter and Co., Berlin

Kelly, J. A., Moews, P. C., Knox, J. R., Frère, J. M., and Ghuysen, J. M. (1982) *Science* **218,** 479–481

Knott-Hunziker, V., Petursson, S., Jayatilake, G. S., Waley, S. G., Jaurin, B., and Grundström, T. (1982) *Biochem. J.* **201,** 621–627

Knox, J. R., DeLucia, M. L., Murthy, N. S., Kelly, J. A., Moews, P. C., Frère, J. M., and Ghuysen, J. M. (1979) *J. Mol. Biol.* **127,** 217–218

Levitt, M., and Chothia, C. (1976) *Nature (Lond.)* **261,** 552–558

Maruyama, I. N., Yamamoto, A., Maruyama, T., and Hirota, Y. (1983) in *The Target of Penicillin* (Hakenbeck, R., Holtje, J. V., and Labischinski, H., eds) pp. 343–402, W. de Gruyter and Co., Berlin

Matthews, B. W. (1966) *Acta Crystallogr. Sect. B Struct. Crystallogr. Cryst. Chem.* **20,** 230–239

Moews, P. C., and Bunn, C. W. (1971) *Acta Crystallogr. Sect. B Struct. Crystallogr. Cryst. Chem.* **27,** 1780–1782

Moews, P. C., Knox, J. R., Waxman, D. J., and Strominger, J. L. (1981) *Int. J. Pept. Protein Res.* **17,** 211–218

Richardson, J. S. (1981) *Adv. Protein Chem.* **34,** 168–339

Schultz, G. E., and Schirmer, R. H. (1979) *Principles of Protein Structure,* pp. 84–85, Springer-Verlag, New York

Sheridan, R. P., and Allen, L. C. (1980) *Biophys. Chem.* **11,** 133–136

Sigler, P. B. (1970) *Biochemistry* **9,** 3609–3617

Spratt, B. G. (1983) *J. Gen. Microbiol.* **129,** 1247–1260

Sykes, R. B., Cimarusti, C. M., Bonner, D. P., Bush, K., Floyd, D. M., Georgopapadakou, N. H., Kester, W. H., Liu, M. C., Parker, W. L., Principe, P. A., Ratnum, M. L., Slusarchyk, L. A., Trejo, W. H., and Wells, T. S. (1981) *Nature (Lond.)* **289,** 590–591

Tomczuk, B. (1980) *Diss. Abstr.* **41,** 576

Tomczuk, B., Kumar, A., Hite, G., Kelly, J. A., Moews, P. C., Knox, J. R., Tilton, R. C., Frère, J. M., and Ghuysen, J. M. (1983) *Abstracts of the Academy of Pharmacological Sciences 35th Meetings, Miami, FL,* p. 172

Waxman, D. J., and Strominger, J. L. (1983) *Annu. Rev. Biochem.* **52,** 825–869

Williams, T. V. (1982) Ph.D. dissertation, University of North Carolina

Yocum, R. R., Rasmussen, J. R., and Strominger, J. L. (1980) *J. Biol. Chem.* **255,** 3977–3986